

## Sintering Crystalline Solids. II. Experimental Test of Diffusion Models in Powder Compacts

R. L. Coble

Citation: *Journal of Applied Physics* **32**, 793 (1961); doi: 10.1063/1.1736108

View online: <http://dx.doi.org/10.1063/1.1736108>

View Table of Contents: <http://scitation.aip.org/content/aip/journal/jap/32/5?ver=pdfcov>

Published by the *AIP Publishing*

---

### Articles you may be interested in

[Analysis of compacted and sintered metal powders by temperature-dependent resistivity measurements](#)

*Appl. Phys. Lett.* **86**, 042114 (2005); 10.1063/1.1857094

[Sintering of crystalline solids: New modelization technics](#)

*AIP Conf. Proc.* **256**, 579 (1992); 10.1063/1.42400

[Shapes of completely wetted two-dimensional powder compacts for applications to sintering](#)

*J. Appl. Phys.* **71**, 3266 (1992); 10.1063/1.350973

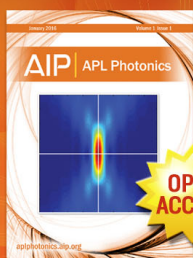
[Mechanical properties and microstructure of sintered PVC powder. II. Permeability and porous structure](#)

*J. Appl. Phys.* **48**, 1902 (1977); 10.1063/1.323896

[Sintering Crystalline Solids. I. Intermediate and Final State Diffusion Models](#)

*J. Appl. Phys.* **32**, 787 (1961); 10.1063/1.1736107

---



## Launching in 2016!

The future of applied photonics research is here

**AIP** | APL  
Photonics

## Sintering Crystalline Solids. II. Experimental Test of Diffusion Models in Powder Compacts

R. L. COBLE

*General Electric Research Laboratory, Schenectady, New York*

(Received December 1, 1960)

During sintering in alumina powder compacts, the density has been found to increase linearly with the logarithm of time, and the grain size increases with the one-third power of time. Incorporation of the time dependence of grain size increase into late-stage bulk diffusion sintering models (from Part I) [R. L. Coble, *J. Appl. Phys.* **32**, 787 (1961)] leads to corrected models by which a semilogarithmic behavior is predicted. The presence of density gradients in normally fabricated pellets makes impossible the deduction of whether theoretical density will be achieved from the early stages of the course of densification. Diffusion coefficients calculated from the intermediate and later stages of sintering bear

order-of-magnitude agreement with those calculated from the initial-stage sintering measurements in alumina. All diffusion coefficients from sintering data are higher than Kingery's measured diffusion coefficients for oxygen. It is hypothesized that the sintering process must then be controlled by bulk diffusion of aluminum ions while the oxygen transport takes place along the grain boundaries. In controlling the sinterability of alumina to theoretical density, it appears that magnesia does not "inhibit" discontinuous grain growth, but instead increases the sintering rate such that discontinuous growth nuclei do not have time to form.

### INTRODUCTION

EXPERIMENTALLY observed densification rates during sintering in powder compacts are nonlinear<sup>1</sup> to the extent that end point densities which vary with temperature have been presumed to exist.<sup>1,2</sup> Quantitative initial-stage sintering experiments<sup>3-5</sup> and qualitative observations in the later stages of sintering suggest that sintering occurs by a diffusion mechanism of material transport.<sup>6,7</sup> Therefore, linear densification rates predicted by diffusion sintering models<sup>8</sup> contrast markedly with the nonlinear rates observed.

Both continuous<sup>9,10</sup> and discontinuous<sup>7,11</sup> grain growth have been observed to occur during sintering. The diffusion models show that the sintering rate is dependent on inverse of grain size to the third power.<sup>12</sup> Therefore, increase in grain size with time would cause the densification rate to decrease with time, as is observed.<sup>1,2</sup> Simultaneous isothermal measurements of density and grain size on a single material are not available in the literature; this paper is a report of such measurements on aluminum oxide samples prepared specifically to evaluate the quantitative applicability of diffusion sintering models (from Part I) to the late stages of sintering in powder compacts.

### EXPERIMENTAL

The samples were prepared from 0.3- $\mu$  alumina powder (Linde A-5175). Some samples were pressed directly from as-received powder. Magnesium oxide was added to others prior to pressing. The magnesia was added as the nitrate to a low-viscosity water suspension of the alumina, mixed in a Waring Blendor. The amount of magnesia added was 0.25 wt%. After mixing, the water was removed by air drying at 200°C. The dried cake which formed was broken up by shaking in a bottle and by hand grinding with a mortar and pestle.

Two forming pressures, 3 and 10 tsi, were employed on different samples to change the green density of the pellets. Pressing was performed in a hardened-steel cylindrical die; lubrication and a double-acting punch operation were employed to minimize axial density gradients. After ejection from the die, the samples were wiped with cellulose tissue to remove the film of discoloration (iron contamination) from the cylindrical surface. Most samples were pressed to a height of 0.4 in.; other heights of 0.2 in. and 0.8 in. were prepared to evaluate the effect of density gradients.

The course of densification during isothermal sintering was determined by three techniques. Sintering in air or oxygen was conducted in a vertical platinum-wound tube furnace which was lightly insulated to allow a rapid heating rate. A single-crystal sapphire rod extended out through the insulation at the top of the furnace. The rod transmitted the movement of the top of the sample on which it was resting to the armature of a differential transformer. The output of the transformer was demodulated and recorded on a strip-chart of a recording microammeter. The transformer was mounted on a platform which could be raised or lowered by a micrometer drive, reading increments of elevation directly to 0.001 in. The apparatus was calibrated for each run by recording the response to 10-mil displacements by the micrometer drive during times before and after the occurrence of rapid shrinkage. Permanent calibra-

<sup>1</sup> P. W. Clark, J. H. Cannon, and J. White, *Trans. Brit. Ceram. Soc.* **52**, 1 (1953).

<sup>2</sup> E. B. Allison and P. Murray, *Acta Met.* **2**, 487 (1954).

<sup>3</sup> G. C. Kuczynski, *Trans. AIME* **185**, 169 (1949).

<sup>4</sup> W. D. Kingery and M. Berg, *J. Appl. Phys.* **26**, 1205 (1955).

<sup>5</sup> R. L. Coble, *J. Am. Ceram. Soc.* **41**, 55 (1958).

<sup>6</sup> B. H. Alexander and R. W. Balluffi, *J. Metals* **2**, 1219 (1950).

<sup>7</sup> J. E. Burke, *J. Am. Ceram. Soc.* **40**, 80-85 (1957).

<sup>8</sup> R. L. Coble, *J. Appl. Phys.* **32**, 787 (1961), preceding paper.

<sup>9</sup> Y. Iida, *J. Am. Ceram. Soc.* **41**, 397 (1958).

<sup>10</sup> J. Belle and B. Lustman, WAPD 184, U. S. Atomic Energy Comm. Research Develop. Rept.

<sup>11</sup> I. Cutler, in *Kinetics of High Temperature Processes*, edited by W. D. Kingery (Technology Press, Cambridge, Massachusetts, and John Wiley & Sons, Inc., New York, 1949).

<sup>12</sup> C. Herring, *J. Appl. Phys.* **21**, 301, 437 (1950).

tion was precluded by the nonlinearity of the response of the transformer and because the rod position could not be exactly reproduced. The samples were supported by a platinum pan on an alumina bubble refractory which extends down through the temperature gradient to a porous insulating fire brick. Two Pt, Pt 10% Rh thermocouples were used, one inside the tube to read the temperature just below the sample, the other outside the tube near a turn of the furnace winding. The latter thermocouple was used for control, at a position where the off-on cycle was short enough to yield less than one degree temperature fluctuation internally and less than  $\frac{1}{2}$ -mil recorded amplitude from expansion and contraction of the push rod. Since the total measured shrinkage was 160 to 200 mils, this contribution to error was smaller than the fluctuations observed ( $\approx 2$ -3 mils) due to daily line-voltage and room-temperature changes.

The samples were placed in position with the furnace at room temperature. The temperature was then raised to about 1050°C and held for at least  $\frac{1}{2}$  hr to allow the system to come to thermal and mechanical equilibrium. This temperature was selected because it was too low for measurable shrinkage to take place within this time interval. The strain-measuring device was calibrated after the system expansion stopped. Power was supplied at the rated maximum current with periodically increased voltage when raising the sample to the test temperature, in order to minimize the time during which nonisothermal shrinkage occurred. In practice, a time interval of 3-5 min was required, the latter being the case for the maximum test temperature; i.e., 1640°C.

Most tests in this apparatus were conducted in ambient air. A few tests were run in flowering oxygen (100 cc/min) admitted through the bore of an alumina thermocouple insulator.

Hydrogen atmosphere shrinkage tests were conducted within alumina (Morgan ΔRR) insert tubes (1-in. i.d.)

in a globar heated furnace. Hydrogen flow rates in excess of 200 cc/min were employed. The sample diameter was measured periodically (after quench heating) by a telescope equipped with a filar micrometer eyepiece. In contrast to the diametral shrinkage measurements recorded manually, the automatically recorded data was of the change in height of samples, i.e., of length change in the direction of pressing. The diametral shrinkage measurements were taken (with the telescope) at a pressed end face of the sample. The dimensions of the samples were measured before and after each shrinkage run. The data are presented as relative density values which were obtained from the measured shrinkage, final length  $L_F$ , and density measurement after sintering. The sample volume was determined from weight change during water (or carbon tetrachloride) displacement. The relative density  $\rho$  at any time is then related to the length  $L$  at any time by the equation

$$\rho = (L_F/L)^3 \rho_F,$$

in which  $\rho_F$  is the relative density of the sample after firing.

In addition to the above techniques by which each isothermal densification curve was made with single samples continuously at temperature, a series of pressed pellets were fired at various times and at different temperatures and with variable forming pressure. The density of each sample was determined directly by gravimetric measurement after cooling to room temperature. Samples were quench heated to the pre-stabilized test temperature in a molybdenum-wound, hydrogen-protected alumina muffle furnace. The series of samples was polished, etched for approximately 5 min with boiling concentrated phosphoric acid, and photographed on a metallograph for grain size determinations.

The grain size was determined by counting the number of grain boundaries intersected by measured lengths of random straight lines drawn directly on the photomicrographs. The grain sizes reported here are equal to 1.5 times the average length between intercepts.

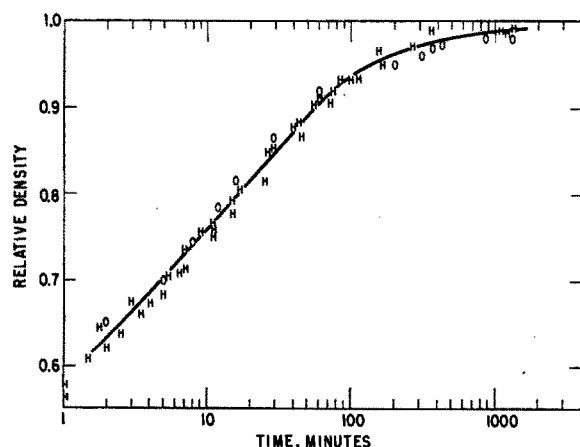


FIG. 1. Densification (calculated from final density and periodic diameter measurements) of several alumina compacts pressed at 10 tsi and heated to 1480°C in oxygen (O) and hydrogen (H), respectively.

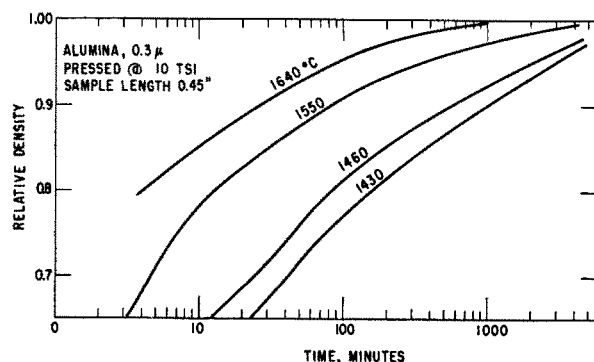
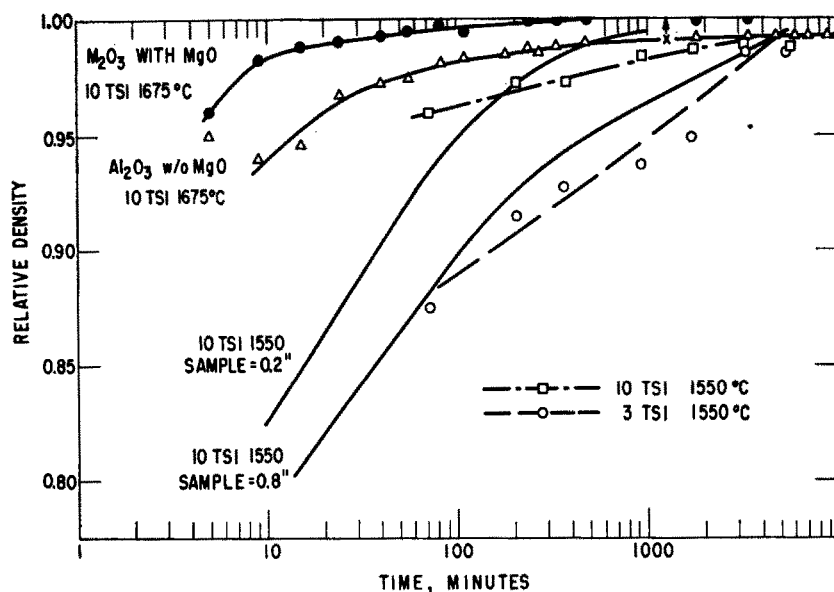


FIG. 2. Densification (calculated from final density and continuous pellet height measurement) of alumina compacts pressed at 10 tsi and heated to several temperatures.

FIG. 3. Densification of alumina compacts illustrating the effects of magnesia additive at 1675°C, sample size at constant forming pressure at 1550°C, and forming pressure at constant size at 1550°C.



### DENSITY RESULTS

Isothermal density:time curves in Figs. 1, 2, and 3 present the effects of atmosphere, temperature, sample size, and forming pressure on the course of densification up to high values of relative density. In addition to the above variables, the different experimental techniques employed are reflected in altered time dependence. The results in Fig. 1 were obtained from diametral-shrinkage and final-density measurements, Figs. 2 and 3 were obtained from height-shrinkage and final-density measurements, while some of the other data in Fig. 3 (plotted as individual points) were obtained from final-density measurements from series of samples.

Comparison of the time dependences in Figs. 1 and 2 reveals differences which are attributed to inhomogeneities in bulk density, in pore size distribution, and in particle alignment. These inhomogeneities lead to shrinkage and shrinkage-rate anisotropy and may be altered by changing forming pressure or sample size. Forming-pressure and size effects on densification rate are presented in Fig. 3. The common density gradient due to die wall friction is present as lower central density. This leads to the hourglass shape when the sample is fired to its limiting density, and also causes the total axial shrinkage to exceed the diametral shrinkage of the pressed face. The greater (initial) density gradient in the axial direction will also cause the sintering rate to decrease as the sample approaches the density limit, because the regions of highest green density require less time to achieve the density limit and then stop shrinking. The successively lower (initial) density planes will reach their density limits and stop shrinking successively. For this reason, the time dependences of shrinkage in the axial and diametral directions are different.

In addition to this end point effect, there is an inter-

mediate-stage rate effect to be associated with the low density in the center of the compact. The lower density must be formed by an increased ratio of average pore size: particle size, by having increased numbers of large pores present. Because the small pores disappear first, with successively larger pores closing consecutively, the shrinkage rate decreases by a larger amount if a wider pore-size distribution is present (as caused by a greater density gradient initially present).

Another important possible sample inhomogeneity is of particle alignment; elongated particles (or agglomerates) tend to become parallel to one another due to pressing operation. The initial sintering rate would then be more rapid in the direction of pressing because there is a larger number of contacts (at which shrinkage occurs) per unit length. Because this effect is opposite to the effect of wider pore-size distributions, the relative rates may vary depending on which predominates. The more rapid axial shrinkage observed suggests that particle alignment is the more important.

Considering these several effects, the greater linearity of the density vs log time presented in Fig. 1, up to ~95% dense compared with the curves in Fig. 2, is attributed to the greater homogeneity of the pressed surface in comparison with the axial direction. The differences in rate due to the gradients cannot now be quantitatively predicted. The inability to rationalize these differences raises the question as to whether direct density measurements on hydrostatically pressed samples (which exhibit isotropic shrinkage) are to be preferred for testing the sintering models. The view taken here is that the isotropic shrinkage merely masks effects of the density gradients in the radial direction, and therefore such samples do not provide better data for either testing the models or for absolute rate calculations. Therefore, the quantitative discrepancy due to

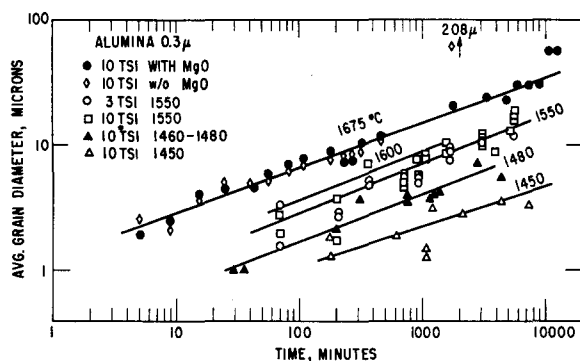


FIG. 4. Grain growth in alumina compacts with temperature, forming pressure, and magnesia additive as variables.

the gradients is considered tolerable, particularly since the effects are qualitatively understood.

### GRAIN GROWTH

The grain sizes of samples fired for various times and temperatures are presented in Fig. 4. There were two series of samples fired at the highest isotherm (1675°C); all samples were pressed at 10 tsi. One series contained  $\frac{1}{4}$  wt. %MgO and is denoted by the filled circles, while the other series was of undoped alumina and is denoted by open diamonds. Both series exhibit normal grain growth up to a size of 10  $\mu$  at 560 min. Beyond this time, the samples containing magnesia continue to exhibit normal growth at the same time dependence, while the undoped specimens undergo discontinuous growth. At 1800 min discontinuous growth is completed and the grain size is 208  $\mu$  in the undoped specimen. Beyond 1800 min the grain size of the undoped specimens was variable but was not observed to fall below 130  $\mu$ .

The effect of changing the initial density by variable forming pressure was determined on samples fired at 1550°C and at 1600°C. Two series of samples were pressed at 3 tsi and 10 tsi, yielding initial densities of 42 and 47% of theoretical, respectively. The grain sizes of the samples fired at 1550°C are individually plotted in Fig. 4 with the denoted forming pressure identified in the key. That the original density difference is maintained through the times when the grain sizes are compared is shown by the data in Table I, in which linear shrinkages and densities of the samples fired at 1550°C are presented. The individual points for the samples fired at 1600°C are omitted to avoid confusion because of scatter and overlap. The results at 1550°C and 1600°C show that the rates of grain growth (at a given temperature) are independent of small differences in volume fraction porosity.

### SLOPES

The curves drawn through the points for the respective isotherms have slopes of 0.36 at 1675°C, 0.39 at 1550°C, 0.37 at 1480°C, and 0.31 at 1450°C. The results for most temperatures other than 1675° include data

collected at various times (i.e., the samples were not prepared and fired in series). The increased scatter suggests possible temperature changes, perhaps due to thermocouple drift. From these data the time dependence of grain growth is taken as simply the  $\frac{1}{3}$  power of time. The occurrence of a continuous simple time dependence for grain growth (such as the  $\frac{1}{3}$  power observed here) is one of the criteria for the identification of "normal" grain growth. Discontinuous growth is identified by the departure from this simple time dependence, illustrated by the behavior of the undoped samples fired at 1675°C (see Fig. 4).

The phenomenological temperature dependence of grain growth evaluated from Fig. 4 will be single valued because the curves are straight and parallel. The rate is evaluated for each temperature by taking the total time at which the respective curves cross the 3- $\mu$  grain size. The reciprocal of the total elapsed time is directly proportional to the rate constant for grain growth; the log of reciprocal time is plotted against reciprocal absolute temperature in Fig. 5. To interpolate for specific grain sizes in calculations of diffusion coefficients from densification tests, the Arrhenius plot along with the observed  $\frac{1}{3}$ -power time dependence of growth was used. The phenomenological activation enthalpy for this temperature dependence of grain growth is  $153 \pm 15$  kcal/mole.

## DISCUSSION

### Time Dependence

The relation derived in Part I for bulk diffusion sintering applicable during the later stages is

$$dP/dt = (ND\gamma a_0^3)/(l^3 kT), \quad (1)$$

in which  $N$  is a numerical constant which equals 10 when the pore phase is a continuous channel on three-grain edges, and equals  $6\pi/2$  when the pore phase is spherical and located at four-grain corners,  $a_0$  is the lattice spacing, and  $k$  is Boltzmann's constant. The isothermal rate of pore volume change ( $dP/dt$ ) is given at constant temperature  $T$ . If  $T$  is fixed, so are the diffusion coefficient  $D$  and the surface energy  $\gamma$ . The

TABLE I. Shrinkages, densities, and grain sizes of alumina samples pressed at 3 and 10 tsi and fired at 1550°C for various times.

Time at 1550°C (min)	$\Delta L/L_0(\%)$		$\rho_b/\rho_t$		G.S. ( $\mu$ )	
	3	10	3	10	3	10
0	0	0	41	47	0.3	0.3
70	19.5	18.7	87.4	96	2.3	2.4
205	20.6	19.8	91.5	97.3	2.9	2.8
370	21.6	20.0	92.7	97.3	4.9	6.2
929	22.1	19.1	93.7	98.4	5.2	6.7
1690	22.7	20.0	95.4	98.8	8.5	9.4 <sup>a</sup>
3135	22.7	20.3	98.5	98.8	10.8 <sup>a</sup>	11.0 <sup>a</sup>
5565	23	20.6	98.7	98.8	12-19 <sup>a</sup>	16.5 <sup>a</sup>

<sup>a</sup> Duplex structures; measured size is of the fine-grained matrix.

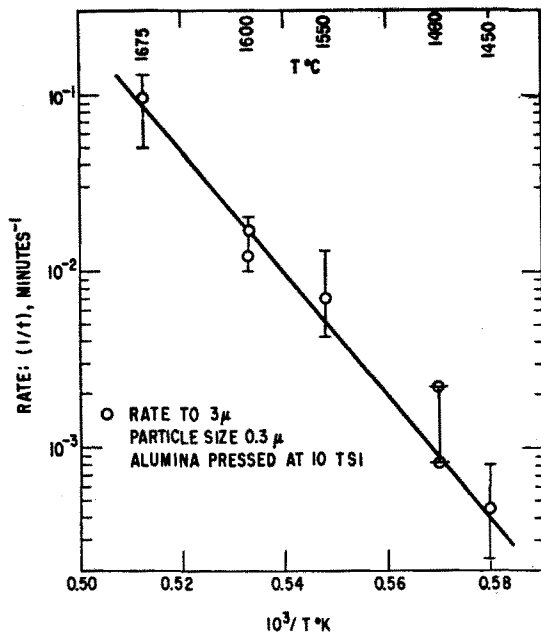


FIG. 5. Logarithm of grain growth rate vs reciprocal temperature.

expressions are applicable over a limited range of density change such that the concomitant change in grain size  $l$  is small or nonexistent. The grain size change with time observed in Fig. 4 can be expressed as

$$G^3 - G_0^3 = At, \quad (2)$$

which may be simplified as  $G^3 = At$  when  $G$  is much larger than  $G_0$ . This can be introduced into the densification equations by calling  $l^3 = G^3 = At$ . Substituting for  $l^3$  yields

$$\frac{dP}{dt} = \frac{ND_\gamma a_0^3}{A_\gamma kT},$$

which integrates to

$$P \Big|_{P_0}^P = \frac{-ND_\gamma a_0^3}{AkT} \ln t \Big|_{t_0}^{t_f}. \quad (3)$$

Thus, upon inserting the grain size dependence on time, the densification rate is predicted to change linearly with log time, as is observed in Figs. 1 and 2. Because of the identical form of the intermediate and final stage models (at high density), the semilogarithmic behavior is valid for either of these stages, but with slightly different numerical constants.

### Slopes

The significance of the slopes of the density vs log time curves is not known. The property to be assessed then, to determine whether the diffusion model is supported, is solely the linearity of the curves as they are presented.

### Linearity

The density-time curves extend through the transition of pore closure and therefore cover both the intermediate and final stages of the process. The gravimetric measurements revealed that in these samples the pore phase becomes completely discontinuous at about 98% of theoretical density, though it begins to change continuity at about 95%. The changes in slope in Figs. 1, 2, and 3 at about 95% are partially attributed to the change in pore phase continuity. Another cause for a change in slope is that in the range from 95–98% density, the equation for densification of closed pores<sup>8</sup> predicts nonlinear time dependence. Another possible cause of the nonlinearity is that gas trapped in the closed pores cannot diffuse out sufficiently rapidly to avoid decreasing the rate of densification. Other effects to which the high-density curvature may be attributed are inhomogeneities initially present in the samples, as discussed above. Which of these effects is responsible for the observed curvature is not known, but because of the multiple effects, the rates at high density are more uncertain than in the range from 80–95% dense.

### Criticality

A general point of interest concerning the density: time curves is whether they reveal the criticality in sintering to theoretical density. The results in Fig. 3 clearly show that the criticality is masked by other larger effects. A series of samples of alumina containing MgO, pressed at 10 tsi and sintered at 1675°C, achieve theoretical density, after  $\approx 250$  min, as shown by data represented by solid circles in Fig. 3. A similar series of samples which did not contain magnesia are represented as open triangles. In the latter series, discontinuous grain growth occurred at the interval  $\approx 1000$  min, denoted by the "X", and remained at 99% dense even after a total time of 10 000 min. The samples which contained magnesia are from 1–2% more dense during this interval beyond 30 min elapsed time. The difference in density is presumed to be due to enhanced sintering rates of alumina by magnesia because the initial densities of the two series were identical. Comparison with the gradient effect illustrated in Fig. 3 reveals larger density differences due to density gradient effects than are present between samples which will and will not sinter to theoretical density during the critical stage of densification. Therefore, the critical effect during sintering to theoretical density cannot be identified from the course of densification. This can be most strikingly illustrated by the fact that the 3-tsi and 10-tsi series, as well as the 0.2-in. and 0.8-in. samples, will all sinter to theoretical density if magnesia is present.

### Temperature Dependence and Convergence

The large observed increase in densification rate with increasing temperature is typical of thermally activated

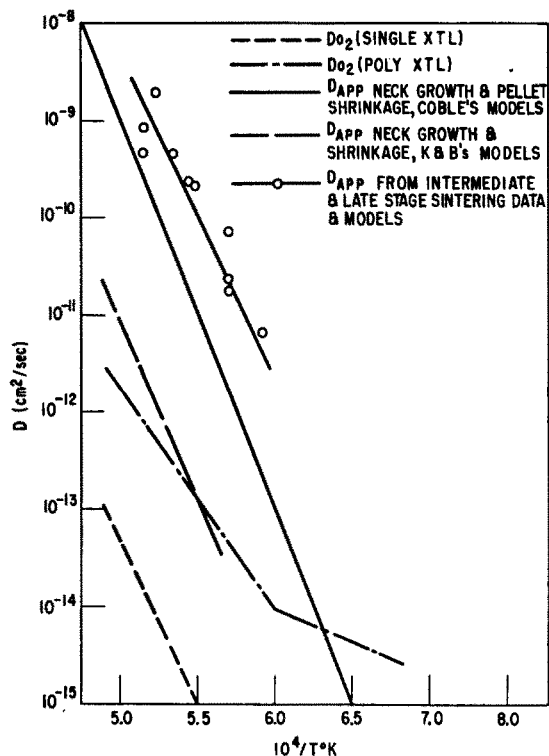


FIG. 6. Diffusion coefficients in alumina versus reciprocal temperature, directly measured oxygen coefficients measured in single-crystal and polycrystalline samples<sup>14</sup> are compared with values calculated from sintering experiments and models.

processes in refractories. Each curve has roughly the same character. The slopes vary, but as was noted above, the slope is not understood, and therefore the change in slope from one curve to another is not understood. It is noteworthy that the curves proceed to theoretical density. This is expected with suitable plotting of diffusion controlled geometric changes for which no end-point density exists. (If a plastic flow mechanism of material transport were operative,<sup>13</sup> yield-point limited end point densities would be predicted.) That theoretical densities have been achieved from samples sintered in the temperature range from  $\approx 1500^{\circ}$ – $1900^{\circ}\text{C}$  with the required times decreasing from days to minutes, respectively, is also taken as evidence that a diffusion mechanism is operative.

*Apparent diffusion coefficients* were calculated from the results shown in Figs. 2 and 3 with Eq. (1). Small intervals of porosity change were selected at a given temperature and the corresponding times were noted, the difference in times giving  $\Delta t$ . (The small interval was deliberately chosen in order to minimize the deviation due to grain growth during the interval.) The grain sizes were taken directly from Fig. 4 or evaluated for the start and finish of the interval for a given temperature and averaged for calculation of the diffusion coefficient. The apparent diffusion coefficients were plotted

in Fig. 6 as  $\log D$  against the reciprocal of absolute temperature. Other data plotted in Fig. 6 are Kingery's<sup>14</sup> directly measured diffusion coefficients for oxygen, and Coble's<sup>5</sup> apparent diffusion coefficients from the initial stage of sintering alumina.

The diffusion coefficients calculated from initial-stage sintering measurements are lower than those from intermediate- and final-stage measurements by one to three orders of magnitude depending on the initial-stage model selected. Only order-of-magnitude reliability may be attached to the individual models or results, and therefore the discrepancy does not disprove that a single mechanism is operative for all these stages. This discrepancy means, however, that a single densification curve by diffusion should not be synthesized from the individual "stage" equations, and that accurate quantitative conclusions about the final densification cannot be drawn from initial stage measurements. Comparison of the apparent diffusion coefficients calculated with Eq. (1) from the data at late stages of sintering with Kingery's oxygen diffusion measurements<sup>14</sup> in alumina single crystals reveals a discrepancy of five orders of magnitude, the calculated coefficients being higher. Kingery's measurements showed that the apparent bulk diffusion coefficient of the oxygen was enhanced by two orders in polycrystalline samples of  $30\text{-}\mu$  grain size in a manner presumed analogous to the enhanced chlorine diffusion coefficient in the vicinity of grain boundaries in NaCl.<sup>15</sup> Because the qualitative aspects of the sintering measurements support a bulk diffusion mechanism, the present data can be rationalized by assuming that sintering is controlled by bulk diffusion of aluminum ions, while the necessary transport of oxygen takes place at grain boundaries. Because the grain sizes in sintering measurements reported here are smaller than in Kingery's oxygen diffusion measurements, further enhancement of apparent oxygen diffusion is possible. The earlier assumption<sup>5,16</sup> that *bulk* diffusion sintering must be controlled by the *slower* diffusing species in the bulk may be overly restrictive if the rate at which the slower diffusion species can move is enhanced by the presence of grain boundaries.

### Time Dependence of Grain Growth

The increase in grain size with time in a normal grain size distribution with no inhibiting second phase has been predicted,<sup>17</sup> and observed in pure systems<sup>18</sup> to follow the square root of time. Most observed growth rates have smaller time dependences than  $t^{1/2}$  however, due to impurities, inclusions, surface effects, etc., which

<sup>14</sup> Y. Oishi and W. D. Kingery, J. Chem. Phys. **33**, 480 (1960).

<sup>15</sup> J. F. Laurent and J. Bénard, Compt. rend. **241**, 1204 (1955).

<sup>16</sup> R. L. Coble in *Kinetics of High Temperature Processes*, edited by W. D. Kingery (Technology Press, Cambridge, Massachusetts, and John Wiley & Sons, Inc., New York, 1959).

<sup>17</sup> P. A. Beck, J. C. Kremer, L. J. Demer, and M. L. Holzworth, Trans. AIME **175**, 372 (1948).

<sup>18</sup> J. E. Burke, Trans. AIME **180**, 173 (1949).

<sup>13</sup> J. K. MacKenzie and R. Shuttleworth, Proc. Phys. Soc. (London) **62**, 360B, 833 (1949).



may also cause a log size:log time plot to be nonlinear. During sintering, most attention has been devoted to discontinuous grain growth<sup>7,11</sup> or to isochronal measurements, with the consequence that isothermal normal grain growth data are rare. Belle and Lustman<sup>10</sup> reported changing rate of growth in sintered  $\text{UO}_2$ . The slopes at 1500° and 1700°C were initially  $\approx 0.67$ –0.9 respectively, and in the 1700°C series the rate slowed down to a slope which could be interpreted as  $\frac{1}{3}$ . The initial slope higher than  $\frac{1}{2}$  cannot be accounted for by a normal growth process but probably is discontinuous growth inhibited by pores. The present determination is that grain growth follows the  $\frac{1}{3}$  power of time during sintering, but the numerical exponent is not understood.

### Temperature Dependence of Grain Growth

The phenomenological temperature dependence of grain growth (153 kcal) was found to be roughly equivalent to the values (150, 145, 165, 125, and 135 kcal top to bottom) for the apparent diffusion coefficients plotted in Fig. 6. Even though the basic mechanisms of grain growth and sintering are different, the comparison shows that their activation enthalpies are equivalent. It is normally assumed<sup>19</sup> that grain growth should exhibit the kinetics of grain boundary diffusion, which for the few cases measured has a lower activation energy than bulk diffusion. The enthalpy equivalence suggests that grain growth is dependent on pore removal, which supports the view<sup>8</sup> that a metastable network of pores and boundaries exists during the intermediate and final stages of sintering.

### Discontinuous Grain Growth

It is important to note that considerable normal grain growth occurs before the limiting density is approached. For instance, the data (in Fig. 4) show that samples containing MgO have grown from 0.3 to  $\approx 9.0 \mu$  at 200 min when they first attain theoretical density (from Fig. 3). The magnesia-free series also exhibited growth by a factor of 30 before discontinuous grain growth occurred. (This geometric change is more than sufficient to permit a metastable structure of boundaries and pore surfaces to form.)

According to the most direct application of Zener's model for particulate inhibition of grain growth,<sup>20</sup> a critical amount of a dispersed phase will inhibit growth locally and permit discontinuous growth nuclei to form in other local regions where growth is permitted. If a larger amount of the dispersed phase were present,

normal growth would be completely inhibited. We are forced to assume then that if discontinuous growth occurs at a "critical" porosity, normal growth should be totally inhibited for all shorter times when the amount of porosity present is larger.

There are two points of importance with respect to the fact that discontinuous growth does not occur when magnesia is present. If discontinuous growth inhibition were caused by a considerable reduction in boundary mobility by either a solid solution mechanism or by the presence of spinel as solid phase inclusions, the rate of normal grain growth should also be inhibited. However, normal grain growth is equivalent in both series prior to discontinuous growth in the undoped series.

Alternatively, the magnesia could change the degree of inhibition by the pore phase. This would result from changes in equilibrium pore shape, which in turn could result from increase in the grain boundary energy:surface energy ratio with magnesia solution. This effect must also be discarded because it should change the rate of normal growth. This may be analogous to the fact that a small change in porosity did not affect the rates of normal growth in otherwise equivalent samples. Further, the series containing MgO fired at 1675° exhibits continuous growth beyond the time when theoretical density is achieved; i.e., any increase in growth rate or departure from  $\frac{1}{3}$ -power time dependence, expected as a result of the disappearance of the inhibiting pore phase, is not observed.

These observations, in addition to the fact that the magnesia-containing series was more dense (by 2%) than the magnesia-free series in the time range just prior to the occurrence of discontinuous growth, suggest that growth is not "inhibited" by the presence of magnesia. It seems more likely that the critical condition for the occurrence of discontinuous growth has been averted by the enhancement of the sintering rate by the presence of the magnesia. If we assume that a "critical density" is present at 99% when the magnesia-free series undergoes discontinuous growth, we may note that the series containing magnesia passes through this region at a decade earlier time. If we next assume that a minimum interval of time for the formation of discontinuous growth nuclei and the subsequent completion of discontinuous growth is manifested in the magnesia-free series, we may conclude that the magnesia-containing series passes through the critical density region so rapidly that there is insufficient time for the formation of discontinuous growth nuclei.

### ACKNOWLEDGMENTS

The author gratefully acknowledges many helpful discussions with J. E. Burke and W. D. Kingery.

<sup>19</sup> D. Turnbull, Trans. AIME **191**, 661 (1951).

<sup>20</sup> C. S. Smith, Trans. AIME **175**, 15 (1948).